Journal of Materials Chemistry C

ROYAL SOCIETY OF CHEMISTRY

PAPER

View Article Online
View Journal | View Issue

Cite this: J. Mater. Chem. C, 2024, 12, 10104

Magnetic anisotropy evolution with Fe content in electrodeposited $Ni_{100-x}Fe_x$ thin films†

A. Begué, [ab] N. Cotón [a] and R. Ranchal *[ac]

In this study, we have experimentally and theoretically determined how the magnetic anisotropy of $Ni_{100-x}Fe_x$ thin films evolves as a function of the Fe content in electrodeposited samples. When the Fe content is below 12 at%, stripe domains are promoted once the thickness exceeds a critical value. For an Fe content of 7 at%, the transcritical shape is present in the hysteresis loop for a thickness of 600 nm. However, for compositions equal to or above 12 at%, we have not found evidence of stripe domains, as indicated by the absence of the transcritical shape in the hysteresis loops for layer thicknesses as high as 1 μm even if a magnetic field is applied perpendicular to the sample plane during growth. All the studied layers are polycrystalline with a ⟨111⟩ texture. The experimental results are understood in the framework of a theoretical model which considers different contributions to the magnetic anisotropy: magnetocrystalline, magnetoelastic, magnetostatic and from pairs. Out-of-plane anisotropy promoted by columnar growth has not been considered as the saccharine-based electrolyte used for the electrodeposition prevents it. In fact, the magnetic anisotropy related to pairs, which is not generally taken into account in models for $Ni_{100-x}Fe_x$, appears to play a crucial role in these thin films. Fitting of the experimental results to this model reveals that the local anisotropy generated by pairs can be as high as 3.30×10^6 J m^{-3}. This theoretical and experimental combined investigation highlights the relevance of all these fundamental mechanisms for the understanding and tuning of magnetic materials.

Received 25th March 2024,
Accepted 4th June 2024

DOI: 10.1039/d4tc01189a

rsc.li/materials-c

1. Introduction

Control of magnetic anisotropy is a key issue when dealing with magnetic materials, and in particular for thin films. While for some applications perpendicular magnetic anisotropy (PMA) is crucial to increase for example the magnetic storage capacity[1–5] or to create spin textures such as skyrmions or stripe domains,[6–9] it might be considered a disadvantage for other applications such as giant magnetoimpedance (GMI) sensors in which the need for soft magnetic properties is crucial.[10–12] Since optimum performance of GMI sensors is obtained for a thickness of around 1 μm, the insertion of layers is required to avoid the formation of stripes once the thickness exceeds the critical value for their formation, which is around 200 nm for sputtered $Ni_{80}Fe_{20}$ layers[11] or even lower for materials with a higher PMA such as FePt.[13] Generally, the presence of stripe domains can be identified in the in-plane (IP) hysteresis loops, which exhibit what it is known as the "transcritical shape",[14–16] characterized by a linear behaviour in the magnetization curve as the magnetic saturated state is reached[14–19] and an increase of coercivity in comparison to thinner samples without stripes.[14]

$Ni_{100-x}Fe_x$ alloys have been broadly studied due to their low coercivity and large saturation magnetization (M_{sat}).[10–12,14,17,18,20] In sputtered $Ni_{80}Fe_{20}$ thin films, the appearance of stripe domains has been previously reported when a certain critical thickness is exceeded due to columnar growth.[10,14] The possibility of avoiding columnar growth through electrodeposition in continuous mode by adding saccharine to the electrolyte has been reported. This addition enables smooth and uniform deposition while preventing columnar growth in NiCu and $Ni_{80}Fe_{20}$ alloys.[21,22] However, in our previous investigation of electrodeposited $Ni_{90}Fe_{10}$ thin films grown from a saccharine-based electrolyte, we have shown that when the electrolyte is not stirred, stripe domains are formed for thicknesses above 0.8 μm.[17] Moreover, when the electrolyte is not stirred and stripes are promoted, the critical thickness for their formation can be reduced if a perpendicular magnetic field to the sample plane is applied during growth.[18]

Here, we have systematically investigated the evolution of the magnetic anisotropy in electrodeposited $Ni_{100-x}Fe_x$ layers obtained from a saccharine-based electrolyte in a compositional range between $7 \leq x \leq 48$ at% Fe. The effect of the thickness and even of a perpendicular magnetic field applied

[a] Dpto. Física de Materiales, Fac. CC. Físicas, Universidad Complutense de Madrid, Ciudad Universitaria s/n, Madrid 28040, Spain. E-mail: rociran@ucm.es
[b] Fac. Ciencias, Universidad de Zaragoza, Zaragoza 50009, Spain
[c] Instituto de Magnetismo Aplicado, UCM-ADIF-CSIC, Las Rozas 28232, Spain

† Electronic supplementary information (ESI) available. See DOI: https://doi.org/10.1039/d4tc01189a

during growth has also been assessed. The interplay between magnetocrystalline, magnetoelastic, magnetostatic and even magnetic anisotropy from pairs plays a crucial role on the evolution of the anisotropy of these ⟨111⟩ textured films.

2. Experimental section

$Ni_{100-x}Fe_x$ layers were grown by electrodeposition on glass substrates covered with a Ti/Au bilayer to increase electrical conductivity. We have used a three-electrode cell with a platinum mesh as a counter electrode and an Ag/AgCl (3 M NaCl) reference electrode. A PalmSens EmStat3+Blue potentiostat was used to perform the depositions at room temperature in non-rotating substrates in a horizontal position. The electrolyte was not magnetically stirred during growth. To deposit the samples, an electric potential of −1.2 V was used. The electrolyte had a fixed composition for H_3BO_3 (0.4 M), $NiSO_4{\cdot}6H_2O$ (0.7 M) and saccharine (17 mM). To tune the $Ni_{100-x}Fe_x$ composition, the concentration of $FeSO_4{\cdot}7H_2O$ ranged from 20 mM to 80 mM.

The growth time of $Ni_{100-x}Fe_x$ was adjusted to reach the expected thicknesses (t) by means of Faraday's law:

$$C = \frac{nFd}{M_{\text{atom}}}St \quad (1)$$

where C is the electric charge measured in the cathode, n is the number of electrons involved in the reduction reaction, F is Faraday's constant (96 485, 34 C mol^{-1}), d is the density of the electrodeposited material, S is the area of the sample, and M_{atom} is the molecular mass. A set of calibration samples was firstly deposited in which the layer thickness was measured by atomic force microscopy (AFM). These samples were used to adjust the formula of Faraday's law to take into account hydrogen evolution.

We have used X-ray diffractometry (XRD) in the Bragg–Brentano configuration to study the structural properties. Measurements were performed using D8 Bruker equipment using the Cu K_α wavelength (λ = 1.54056 Å). The composition of the alloys was measured by energy-dispersive X-ray spectroscopy using JEOL JSM 7600F equipment at 15 kV. In-plane hysteresis loops were measured using a homemade magneto-optical Kerr effect (MOKE) setup in the longitudinal configuration, employing p-polarized light from a laser with a wavelength of 650 nm operating at 10 kHz.

3. Experimental results

The IP hysteresis loops shown in Fig. 1a for $Ni_{93}Fe_7$ layers with thicknesses ranging from 600 nm to 1.4 μm exhibit the transcritical shape, consistent with our previous results on $Ni_{90}Fe_{10}$ films where stripe domains are promoted when deposition is performed under non-stirring conditions.[17] MOKE hysteresis loops appear reversed due to the inversion in Kerr signal promoted by Ni.[23] However, IP hysteresis loops do not exhibit the transcritical shape related to the presence of stripe domains even when the thickness is as high as 1.4 μm if the Fe content increases to 12 at% (Fig. 1b).

Upon comparing 1 μm thick layers with different compositions, it is evident that the transcritical shape is not present once the Fe content is equal to or higher than 12 at% (Fig. 2a). In the $Ni_{90}Fe_{10}$ layers electrodeposited from a saccharine-based electrolyte, we have previously reported that the formation of stripe domains can be enhanced by applying an external magnetic field perpendicular to the sample plane.[18] However, for $Ni_{80}Fe_{20}$ this procedure is not effective even when the layer thickness is 1 μm (Fig. 2b).

To understand the evolution of the magnetic anisotropy in these $Ni_{100-x}Fe_x$ alloys, XRD characterization was performed (Fig. 3a). All the layers exhibit an fcc crystal structure as revealed by the diffraction peaks present in all the patterns which is in agreement with the fact that that this crystal structure is kept up to an Fe content as high as *ca.* 90 at% in $Ni_{100-x}Fe_x$ alloys.[20] In addition, all the studied thin films exhibit a ⟨111⟩ texture regardless of the composition. Therefore, the evolution of the magnetic anisotropy appears to be strongly dependent on the Fe content that controls the formation of stripe domains in electrodeposited $Ni_{100-x}Fe_x$ films being not possible to achieve its formation for compositions equal to or above 12 at%. We have studied the correlation between Fe content and the coherent domain size (D) by means of Scherrer's formula:[24]

$$D = \frac{\gamma}{\text{FWHM}\cos\theta} \quad (2)$$

where γ is a dimensionless factor that depends on the experimental technique and it is generally considered as 0.9, FWHM is

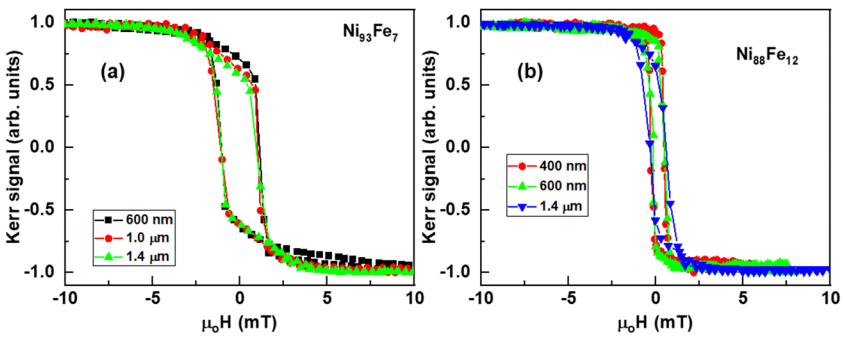

Fig. 1 (a) MOKE hysteresis loops for $Ni_{93}Fe_7$ layers with different thicknesses: (■) 600 nm, (●) 1 μm, and (▲) 1.4 μm. (b) MOKE hysteresis loops for $Ni_{88}Fe_{12}$ layers with different thicknesses: (●) 400 nm, (▲) 600 nm, and (▼) 1.4 μm.

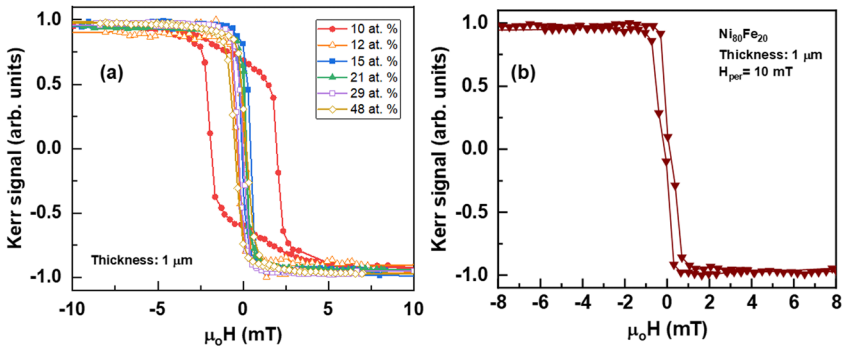

Fig. 2 (a) MOKE hysteresis loops for 1 μm thick $Ni_{100-x}Fe_x$ layers with different Fe contents indicated in the label. (b) MOKE hysteresis loop for a 1 μm thick $Ni_{80}Fe_{20}$ layer deposited under an applied magnetic field of 10 mT perpendicular to the sample plane.

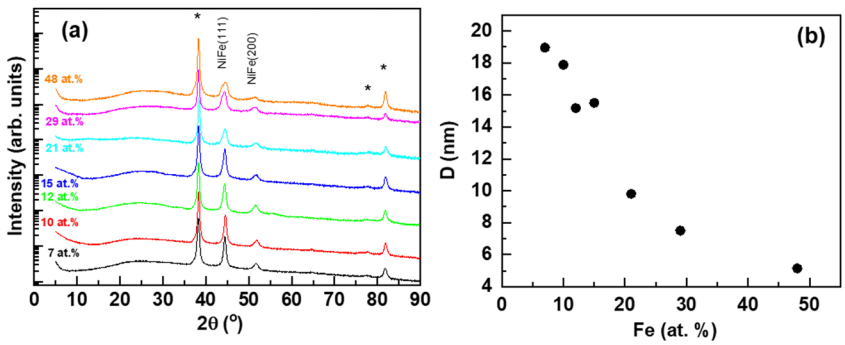

Fig. 3 (a) XRD diffraction patterns for different electrodeposited $Ni_{100-x}Fe_x$ layers. Curves have been vertically shifted for clarity. * is used to indicate peaks related to the Au layer. (b) Coherent domain size (D) inferred from Scherrer's equation as a function of the Fe content.

the full width at half maximum obtained from the fit of the diffraction peak, and θ is the angle at which the diffraction peak is centered. In this study, the diffraction peak related to the reflection (111) has been used to calculate D with eqn (2) in all cases. As presented in Fig. 3b, the coherent domain size strongly decreases with the Fe content indicating that the order inside the Ni matrix is gradually reduced upon Fe introduction. This is the experimental reason for introducing the magnetic anisotropy term related to pairs in the theoretical model, as explained below.

4. Theoretical model

To explain the loss of domain stripes occurring around Fe 12 at%, we have developed a model based on the magnetic anisotropies involved in these alloys. The sign of the total anisotropy of the films is defined taking into account that the magnetocrystalline anisotropy constant is typically defined as $K_1 < 0$ when the magnetization lies along the $\langle 111 \rangle$ directions, and $K_1 > 0$ for perpendicular directions (*i.e.* $\langle 100 \rangle$ direction).[20] From MOKE loops we see that for compositions below Fe 12 at%, the anisotropy is negative, as the magnetization points in the out-of-plane (OOP) direction, which is parallel to the $\langle 111 \rangle$ direction in these textured films. On the other hand, for compositions equal to or above Fe 12 at%, the anisotropy has to be positive as the magnetization lies in the sample plane.

The total magnetic anisotropy, K_{total}, of the films is the sum of the different anisotropies involved:

$$K_{total} = K_{mc} + K_{me} + K_{ms} + K_{pairs} \quad (3)$$

where K_{mc} is the magnetocrystalline anisotropy, K_{me} is the magnetoelastic anisotropy, K_{ms} is the magnetostatic anisotropy and K_{pairs} is the anisotropy generated by pairs. Fig. 4a shows the contribution of each magnetic anisotropy as a function of the Fe content. It is worth noting that, while in magnetoelastic materials, both magnetoelastic and magnetocrystalline anisotropy might be expected to be the most significant, this figure illustrates the contribution of all terms of anisotropy considered in this study for clarity.

K_{mc} is determined by the values of anisotropy constant K_1 for each composition of the $Ni_{100-x}Fe_x$ alloy, with no consideration of K_2 due to its low contribution to the anisotropy. We have introduced in our calculation the data of K_1 for every composition reported by Cullity.[20]

K_{me} is calculated as:

$$K_{me} = \frac{3}{2}\lambda_p \epsilon Y \quad (4)$$

where λ_p is the magnetostriction of the polycrystalline $Ni_{100-x}Fe_x$, ϵ is the microstrain and Y is the Young's modulus. The value of λ_p can be obtained as the average of random orientations of the grains, which depend on the magnetostriction

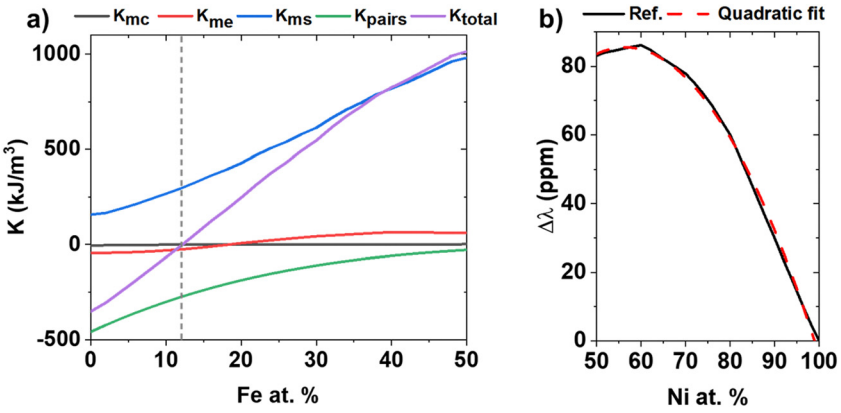

Fig. 4 (a) Dependency of the different magnetic anisotropies with respect to Fe content (at%). The dashed line at Fe 12 at% indicates the change of sign in K_{total}. (b) Excess magnetostriction ($\Delta\lambda$) obtained from the references (black)[20] with its quadratic fit (dashed-red).

constants λ_{100} and λ_{111} for each composition. It is calculated as $\lambda_p = (2\lambda_{100} + 3\lambda_{111})/5$.[20] The microstrain is determined by applying the Williamson–Hall method to the (111) XRD peak as $\epsilon = \mathrm{FWHM}/(4\tan\theta)$.[24] From the values of ϵ obtained at each composition, we performed a linear fit in order to extrapolate the values of ϵ to compositions for which we do not have data (see ESI†). The Young's modulus for each $Ni_{100-x}Fe_x$ composition is obtained from the literature.[25]

Due to the shape of the samples, there is a significant magnetostatic anisotropy leading the magnetization to lie in the sample plane of the thin films. The magnetostatic anisotropy for a film is calculated as:

$$K_{ms} = \frac{1}{2}\mu_0 M_s^2 \quad (5)$$

where μ_0 is the permeability of the vacuum and M_s is the saturation magnetization, which is also obtained from the literature for every $Ni_{100-x}Fe_x$ composition.[20]

In many metallic alloys, there is also a non-negligible contribution to the magnetic anisotropy due to the formation of pairs, denoted as K_{pairs} in this work. Chikazumi already reported that in $Ni_{100-x}Fe_x$ alloys featuring the Ni_3Fe superlattice, the anisotropy exhibits a decrease in its value[26] that is attributed to the ordered superlattice, while disordered configurations, where Fe or Ni atoms are first neighbors, serve to enhance a local uniaxial anisotropy along the direction of pair formation.[27] For other Fe-based alloys such as FeGa, Cullen *et al.* developed a model to calculate the induced anisotropy by pairs, resulting in 5×10^7 J m^{-3} for Ga-pairs in the Fe matrix.[28] This Cullen's model is based on the premise that the excess magnetostriction, $\Delta\lambda$, depends quadratically on the composition. In the studied $Ni_{100-x}Fe_x$ alloys, the addition of Fe to the Ni matrix results in a reduction in coherence length as shown in the reduction of the crystallite size with increasing Fe atomic content (Fig. 3b). The introduction of Fe atoms diminishes this magnetic anisotropy within the Ni matrix, resulting in a reduction of local uniaxial anisotropy. By adapting the model initially formulated for Ga-pairs by Cullen to Ni-pairs, we can effectively express the observed excess magnetostriction:

$$\Delta\lambda = \left(\frac{3}{2}\right) \cdot (\lambda_p - \lambda_{p,Ni}) \quad (6)$$

$\lambda_{p,Ni}$ being the magnetostriction of the polycrystalline Ni. Fig. 4b shows how $\Delta\lambda$ fits the trend of a quadratic dependence with Ni at% indicating that we can actually consider Cullen's model to be applicable to our $Ni_{100-x}Fe_x$ thin films. Then, the calculation of the effective magnetic anisotropy generated by pairs is as follows:

$$K_{pairs} = -\frac{4K^2C^4a^2}{\pi A_0} \quad (7)$$

where K is the local uniaxial anisotropy generated by pairs, C is the Ni atomic content, a is the defect dimension (roughly twice the unit cell unit) and A_0 is the exchange stiffness constant. By using the known values for Ni, such as $a = 0.7$ nm and $A_0 = 15$ pJ m^{-1} we can estimate the value of K that corresponds to the change in sign in K_{total} for Fe at 12 at% (Fig. 4a). The obtained fitted value is $K = 3.30 \times 10^6$ J m^{-3}, which is pretty close to $Fe_{40}Pt_{60}$, 7×10^6 J m^{-3}.[29] Therefore, the theoretical model proposed in this work that takes into account the magnetocrystalline, magnetoelastic, magnetostatic and pair properties enables an understanding of the evolution of the magnetic anisotropy experimentally observed in $Ni_{100-x}Fe_x$ thin films electrodeposited from a saccharine-based electrolyte in which columnar growth is prevented. In fact, at the beginning of this study we also examined the potential role of columnar growth as a source of OOP magnetic anisotropy. As shown in the ESI,† accounting for this contribution shifts the crossover point of the total magnetic anisotropy to a Fe content of 19 at%, which significantly differs from our experimental observations. Consequently, columnar growth is not included in our theoretical model.

5. Conclusions

In conclusion, this study has provided valuable insights into the evolution of the magnetic anisotropy in electrodeposited $Ni_{100-x}Fe_x$ alloys across a range of Fe contents spanning from 7 to 48 at%. Regardless of the composition, all the layers are

polycrystalline with a ⟨111⟩ texture. We have developed a theoretical model for the magnetic anisotropy evolution that accounts for the observed experimental results obtained in a saccharine-based electrolyte in which columnar growth is avoided. Our research underscores the complex interplay between composition, crystalline structure, and different sources of magnetic anisotropies as: magnetocrystalline, magnetoelastic, magnetostatic and from pairs. By elucidating these relationships, we advance our understanding of the fundamental mechanisms governing magnetic behavior in thin films. Due to the use of a saccharine-based electrolyte for the layer growth, the contribution from columnar growth has not been considered. Further research could explore the generalization of the model to magnetic systems where this constraint does not apply, such as in $Ni_{100-x}Fe_x$ sputtered layers.[10,14]

Data availability

The data that support the findings of this study are available from the corresponding author upon reasonable request.

Author contributions

A. Begué: investigation; methodology; writing – original draft; writing – review & editing. N. Cotón: investigation; data curation; validation; writing – review & editing. R. Ranchal: conceptualization; methodology; funding adquisition; supervision; writing – review & editing.

Conflicts of interest

There are no conflicts of interest to declare.

Acknowledgements

This work has been financially supported through the project PID2021-122980OB-C51 (AEI/FEDER) of the Spanish Ministry of Science and Innovation. A. B. would like to acknowledge the funding received from the Ministry of Universities and the European Union-Next Generation for the Margarita Salas fellowship. We thank CNME at UCM for the use of JEOL JSM 7600F, and CAI Difracción de rayos-X at UCM for XRD measurements, respectively.

References

1 B. Dieny and M. Chshiev, Perpendicular magnetic anisotropy at transition metal/oxide interfaces and applications, *Rev. Mod. Phys.*, 2017, **89**, 025008.
2 R. Sbiaa, H. Meng and S. N. Piramanayagam, Materials with perpendicular magnetic anisotropy for magnetic random access memory, *Phys. Status Solidi RRL*, 2011, **5**, 413–419.
3 C. A. Brondin, S. Ghosh, S. Debnath, F. Genuzio, P. Genoni, M. Jugovac, S. Bonetti, N. Binggeli, N. Stojić, A. Locatelli and T. O. Menteş, Tailoring Magnetic Anisotropy in Ultrathin Cobalt by Surface Carbon Chemistry, *Adv. Electron. Mater.*, 2024, **10**, 2300579.
4 K. Wang, X. Fu, L. Yu, Z. Guo, J. Liu, G. Jagadish Kumar and R. Xiong, Perpendicular magnetic anisotropy properties of Co_2FeSi/Pt multilayers deposited on amorphous dielectric Ta_2O_5, *Mater. Sci. Eng., B*, 2024, **301**, 117173.
5 S. Bhatti, R. Sbiaa, A. Hirohata, H. S. Fukami and S. N. Piramanayagam, Spintronics based random access memory: a review, *Mater. Today*, 2017, **20**, 530–548.
6 Y.-C. Li, Y.-H. Huang, C.-C. Huang, Y.-T. Liu and C.-F. Pai, Field-free switching in symmetry-breaking multilayers: the critical role of interlayer chiral exchange, *Phys. Rev. Appl.*, 2023, **20**, 024032.
7 R. Wiesendanger, Nanoscale magnetic skyrmions in metallic films and multilayers: a new twist for spintronics, *Nat. Rev. Mater.*, 2016, **1**, 16044.
8 D. Petti, S. Tacchi and E. Albisetti, Review on magnonics with engineered spin textures, *J. Phys. D: Appl. Phys.*, 2022, **55**, 293003.
9 S. Luo, M. Song, X. Li, Y. Zhang, J. Hong, X. Yang, X. Zou, N. Xu and L. You, Reconfigurable Skyrmion Logic Gates, *Nano Lett.*, 2018, **18**, 1180–1184.
10 E. Fernández, A. V. Svalov, G. V. Kurlyandskaya and A. Garcia-Arribas, GMI in nanostructured FeNi/Ti multilayers with different thicknesses of the magnetic layers, *IEEE Trans. Magn.*, 2013, **49**, 18–21.
11 G. V. Kurlyandskaya, A. V. Svalov, E. Fernandez, A. Garcia-Arribas and J. M. Barandiaran, FeNi-based magnetic layered nanostructures: Magnetic properties and giant magnetoimpedance, *J. Appl. Phys.*, 2010, **107**, 09C502.
12 M. A. Corrêa, F. Bohn, C. Chesman, R. B. da Silva, A. D. C. Viegas and R. L. Sommer, Tailoring the magnetoimpedance effect of NiFe/Ag multilayer, *J. Phys. D: Appl. Phys.*, 2010, **43**, 295004.
13 N. R. Álvarez, J. E. Gómez, A. E. Moya Riffo, M. A. Vicente Álvarez and A. Butera, Critical thickness for stripe domain formation in FePt thin films: Dependence on residual stress, *J. Appl. Phys.*, 2016, **119**, 083906.
14 M. Romera, R. Ranchal, D. Ciudad, M. Maicas and C. Aroca, Magnetic properties of sputtered Permalloy/molybdenum multilayers, *J. Appl. Phys.*, 2011, **110**, 083910.
15 A. Hubert and R. Schäfer, *Magnetic domains*, Springer, 2011.
16 N. Saito, H. Fujiwara and Y. Sugita, A New Type of Magnetic Domain Structure in Negative Magnetostriction Ni-Fe Films, *J. Phys. Soc. Jpn.*, 1964, **19**, 1116–1125.
17 N. Cotón, J. P. Andrés, E. Molina, M. Jaafar and R. Ranchal, Stripe domains in electrodeposited $Ni_{90}Fe_{10}$ thin films, *J. Magn. Magn. Mater.*, 2023, **565**, 170246.
18 N. Cotón, J. P. Andrés, M. Jaafar, A. Begué and R. Ranchal, Tuning the out-of-plane magnetic textures of electrodeposited $Ni_{90}Fe_10$ thin films, *J. Appl. Phys.*, 2024, **135**, 093905.
19 M. Coïsson, G. Barrera, F. Celegato and P. Tiberto, Rotatable magnetic anisotropy in $Fe_{78}Si_9B_{13}$ thin films displaying stripe domains, *Appl. Surf. Sci.*, 2019, **476**, 402–411.
20 B. D. Cullity, in *Introduction to magnetic materials*, ed. C. D. Graham, IEEE/Wiley, Hoboken, N.J, 2nd edn, 2009.

21 M. Troyon and L. Wang, Influence of saccharin on the structure and corrosion resistance of electrodeposited multilayers, *Appl. Surf. Sci.*, 1996, **103**, 517–523.
22 A. Kotelnikova, T. Zubar, T. Vershinina, M. Panasyuk, O. Kanafyev, V. Fedkin, I. Kubasov, A. Turutin, S. Trukhanov, D. Tishkevich, V. Fedosyuk and A. Trukhanov, The influence of saccharin adsorption on NiFe alloy film growth mechanisms during electrodeposition, *RSC Adv.*, 2022, **12**, 35722–35729.
23 A. Green and B. W. J. Thomas, A simple hysteresis loop plotter using the transverse Kerr effect, *J. Sci. Instrum.*, 1966, **43**, 399–401.
24 V. D. Mote, Y. Purushothani and B. N. Dole, Williamson-Hall analysis in estimation of lattice strain in nanometer-sized ZnO particles, *J. Theor. Appl. Phys.*, 2012, **6**, 6.
25 H. M. Ledbetter and R. P. Reed, Elastic Properties of Metals and Alloys, I. Iron, Nickel, and Iron-Nickel Alloys, *J. Phys. Chem. Ref. Data*, 1973, **2**, 531–618.
26 S. Chikazumi, Ferromagnetic Properties and Superlattice Formation of Iron-Nickel Alloys (II), *J. Phys. Soc. Jpn.*, 1950, **5**, 333–338.
27 S. Chikazumi and T. Oomura, On the Origin of Magnetic Anisotropy Induced by Magnetic Annealing, *J. Phys. Soc. Jpn.*, 1955, **10**, 842–849.
28 J. Cullen, P. Zhao and M. Wuttig, Anisotropy of crystalline ferromagnets with defects, *J. Appl. Phys.*, 2007, **101**, 123922.
29 K. Inoue, H. Shima, A. Fujita, K. Ishida, K. Oikawa and K. Fukamichi, Temperature dependence of magnetocrystalline anisotropy constants in the single variant state of L1-type FePt bulk single crystal, *Appl. Phys. Lett.*, 2006, **88**, 102503.